30 December 1994

ELSEVIER

Chemical Physics Letters 231 (1994) 387–394

CHEMICAL PHYSICS LETTERS

The Vegard–Kaplan band and the phosphorescent decay of N_2

Jeppe Olsen [a], Boris Minaev [b], Olav Vahtras [b], Hans Ågren [b], Poul Jørgensen [c], Hans Jørgen Aa. Jensen [d], Trygve Helgaker [e]

[a] *Theoretical Chemistry, Chemical Centre, University of Lund, P.O. Box 124, S-221 00 Lund, Sweden*
[b] *Department of Physics and Measurement Technology, University of Linköping, S-581 83 Linköping, Sweden*
[c] *Department of Chemistry, Aarhus University, DK-8000 Aarhus C, Denmark*
[d] *Department of Chemistry, Odense University, DK-5230 Odense M, Denmark*
[e] *Department of Chemistry, University of Oslo, Box 1033, Blindern, N-0315 Oslo 3, Norway*

Received 21 January 1994; in final form 3 November 1994

Abstract

The phosphorescence transition $A\,^3\Sigma_u^+ \rightarrow X\,^1\Sigma_g^+$ in N_2 is studied by quadratic response and multi-configuration self-consistent field theory. Using full valence correlation reference wavefunctions, response theory predicts the total radiative lifetime of the $(v'=0)\,A\,^3\Sigma_{u,1}^+$ state (the $\Sigma=1$ component) to 2.58 s and the corresponding averaged radiative lifetime to 3.87 s, to be compared with the experimental averaged value of 1.9 s. Though there is a systematic overestimation of the lifetime, the theoretical phosphorescence transition moment curve and the relative vibronic intensities are in good agreement with experiment. A novel derivation of the relation between an induced transition moment and a residue of the quadratic response function is presented.

1. Introduction

In the last decade a number of relativistic effects have been analyzed by ab initio methods (see, for example, Ref. [1]). For molecules consisting of first and second row atoms, the use of the full Breit–Pauli Hamiltonian as a perturbation has allowed successful descriptions of many effects arising from spin–orbit coupling (SOC). Most ab initio SOC calculations have concerned spin–orbit splittings in spectra and intersystem crossings. The recent work of Manaa and Yarkony [2] on the intersystem crossing in the reaction $CH(X\,^2\Pi)+N_2(X\,^1\Sigma_g^+)\rightarrow HCN(X\,^1\Sigma^+)+N(^4S)$ exemplifies the potential of the current methods.

Phosphorescence transitions (delayed emission with radiative lifetime of the order of about 1 s) have also received attention. In phosphorescence a dipole transition occurs between two states of different spin multiplicity, typically between a singlet and a triplet state. This transition is forbidden in the non-relativistic approximation, but the SOC mixes the spin multiplicities and gives a non-vanishing matrix element. Because of high anisotropy of the SOC in molecules, each spin sublevel of the triplet state is associated with a specific transition probability. In diatomics the orbitally non-degenerate triplet state $^3\Sigma$ has two distinct radiative lifetimes associated to the spin sublevels $\Sigma=0$ (spin projection on the internuclear axis) and $|\Sigma|=1$, respectively. In light molecules this state usually belongs to Hund's case (b).

There have been some theoretical studies of phosphorescence transitions [3–5]. A typical approach has been to describe the spin–orbit perturbations in terms of a selected set of intermediate states and performing explicit summations over the intermediate states. In a paper by Langhoff and Davidson [3], it was noted that to obtain a converged phosphores-

SSDI 0009-2614(94)01300-4

cence transition moment for formaldehyde, it was not sufficient to include the lowest 100 states. Manaa and Yarkony [4] employed a state averaged multi-configurational self-consistent field (MCSCF) method followed by second-order configuration interaction to describe the unperturbed states and perturbation theory in the second-order configuration interaction (CI) space to describe the spin–orbit mixings of the states. In this way, they were able to reproduce the experimental intensities for the $a\,^3\Sigma_1^+ \rightarrow X\,^1\Sigma^+$ transition in NO^+. This approach seems, however, hardly feasible for large systems, where phosphorescence is especially important.

An alternative approach is to employ response theoretical methods to calculate phosphorescence transition moments [5]. At the MCSCF level of theory, the response method employs the operators associated with orbital- and CI relaxation to describe the effect of an external perturbation [6]. By also allowing the orbitals to relax in the response to the external field, the requirements to the CI expansion are reduced. MCSCF response theory has in this way successfully described linear and non-linear polarizabilities employing rather modest MCSCF expansions, see for example Ref. [7]. We have previously shown that the phosphorescence transition moment can be identified as a residue of a quadratic response function [6], and have devised computational procedures [5,8] allowing large scale MCSCF calculations of this quantity by employing integral and correlation direct methods. In consistence with other recent work, both the one- and two-body parts of the spin–orbit operator are included.

In this Letter we will use the MCSCF response theory to study the phosphorescence transition $A\,^3\Sigma_u^+ \rightarrow X\,^1\Sigma_g^+$ in N_2. The vibrational–rotational bands corresponding to this electronic transition constitute the Vegard–Kaplan band system which is important for auroral studies and laboratory work involving active nitrogen [9–15]. The present study seems to be the first theoretical examination of the intensities of the Vegard–Kaplan band and the lifetime of the $A\,^3\Sigma_u^+$ state. In Section 2 we present an alternative derivation of the relation between the intensity of an induced transition and the residue of a quadratic response function. Section 3 contains details of the calculations, and Section 4 the numerical results and a discussion. A summary is given in the last section, Section 5.

2. Induced transitions

In this section we give a very direct derivation of perturbation induced transition matrix elements from response function theory. We assume that the transition matrix element $\langle 0|A|n\rangle$ vanishes for the unperturbed system where $|0\rangle$ is the unperturbed reference state and $|n\rangle$ an excited state. Let $|0(\lambda)\rangle$ be the reference state corresponding to the Hamiltonian $H_0 + \lambda W$ where W is a static perturbation. If we add a time-dependent perturbation V, the reference state is changed into $|\tilde{0}(\lambda)\rangle$, and the expectation value of an arbitrary operator A can be written as

$$\langle \tilde{0}(\lambda)|A|\tilde{0}(\lambda)\rangle = \langle 0(\lambda)|A|0(\lambda)\rangle + \int d\omega \exp[-i(\omega+i\epsilon)t] \ll A; V \gg (\lambda)_\omega + \ldots . \quad (1)$$

In Eq. (1), ϵ is a positive infinitesimal ensuring that the time-dependent perturbation is absent at $t = -\infty$ and $\ll A; V \gg (\lambda)_\omega$ is the linear response function at frequency ω. The linear response function depends on the strength λ of the static perturbation, since it is evaluated with $|0(\lambda)\rangle$ as the reference function and $H_0 + \lambda W$ as the zeroth-order Hamiltonian.

It is known from the theory of linear response functions [6] that the transition moments between the reference state $|0(\lambda)\rangle$ and another eigenstate $|n(\lambda)\rangle$ of $H_0 + \lambda W$ can be identified from the residue

$$\lim_{\delta \rightarrow 0} \delta \ll A; V \gg (\lambda)_{\omega_n(\lambda)+\delta} = \langle 0(\lambda)|A|n(\lambda)\rangle \langle n(\lambda)|V|0(\lambda)\rangle , \quad (2)$$

where $\omega_n(\lambda)$ is the transition energy from state $|0(\lambda)\rangle$ to state $|n(\lambda)\rangle$. The differentiation of Eq. (2) with respect to λ gives

$$\frac{d}{d\lambda} \langle 0(\lambda)|A|n(\lambda)\rangle \langle n(\lambda)|V|0(\lambda)\rangle = \lim_{\delta \rightarrow 0} \delta \frac{\partial}{\partial \lambda} \ll A; V \gg (\lambda)_{\omega_n(\lambda)+\delta} + \lim_{\delta \rightarrow 0} \delta \frac{\partial}{\partial \omega} \ll A; V \gg (\lambda)_\omega \frac{d\omega_n(\lambda)}{d\lambda}\bigg|_{\omega=\omega_n(\lambda)+\delta} , \quad (3)$$

where the last term vanishes as it contains the matrix element $\langle 0|A|n\rangle$.

In order to identify $(\partial/\partial\lambda)\ll A; V\gg(\lambda)_\omega$ we repartition the Hamiltonian so that H_0 is the unperturbed Hamiltonian and $\lambda W+V$ is the perturbation. The perturbed wavefunction is still $|\tilde{0}(\lambda)\rangle$ and the expectation value of A can be expanded in response functions as

$$\langle\tilde{0}(\lambda)|A|\tilde{0}(\lambda)\rangle = \langle 0|A|0\rangle + \int d\omega \exp[-i(\omega+i\epsilon)t]\ll A; V\gg_\omega + \lambda\ll A; W\gg_0 + \lambda\int d\omega \exp[-i(\omega+i\epsilon)t]\ll A; V, W\gg_{\omega,0} + \ldots . \quad (4)$$

The above response functions correspond to the unperturbed Hamiltonian H_0. The expansions in Eqs. (1) and (4) must be identical in each order of λ and V. We have therefore the identifications at $\lambda=0$,

$$\frac{\partial}{\partial\lambda}\langle 0(\lambda)|A|0(\lambda)\rangle\Big|_{\lambda=0} = \ll A; W\gg_0 , \quad (5)$$

$$\frac{\partial}{\partial\lambda}\ll A; V\gg(\lambda)_\omega\Big|_{\lambda=0} = \ll A; V, W\gg_{\omega,0} . \quad (6)$$

Inserting Eq. (6) in Eq. (3) gives

$$\frac{d}{d\lambda}\langle 0(\lambda)|A|n(\lambda)\rangle\langle n(\lambda)|V|0(\lambda)\rangle\Big|_{\lambda=0} = \lim_{\delta\to 0}\delta\ll A; V, W\gg_{\omega_n+\delta,0} . \quad (7)$$

Using that $\langle 0|A|n\rangle$ is zero gives that the induced transition matrix element is

$$\frac{d}{d\lambda}\langle 0(\lambda)|A|n(\lambda)\rangle\Big|_{\lambda=0} = \frac{1}{\langle n|V|0\rangle}\lim_{\delta\to 0}\delta\ll A; V, W\gg_{\omega_n+\delta,0} . \quad (8)$$

The residue of the quadratic response function can then be obtained from Ref. [7] giving directly the conventional expressions for the induced transition matrix element.

We will not go into any details about the actual evaluation of the residue of the quadratic response function at the MCSCF level of theory. Refs. [5,8] contain plenty of formulae for elucidating this point.

3. Calculations

An MCSCF response calculation of the phosphorescence transition moment consists of several steps. The ground state is first obtained from an MCSCF optimization. The excited triplet state is then obtained from a linear response calculation with an effort that is comparable to solving one set of linear response equations. To obtain the response of the ground and excited state to the SOC perturbation requires the solution of two sets of linear response equations. A term corresponding to the third derivative of the MCSCF energy with respect to changes of orbitals and CI coefficients is finally evaluated.

Although the use of response methods avoids the explicit construction of excited states, it is necessary that the excited state can be described in terms of orbital- and CI-excitation operators working on the reference state. In the present case, the excited triplet state is dominated by the $1\pi_u^3 1\pi_g$ configuration which is obtained from a single excitation from the ground state $1\pi_u^4$ configuration and therefore well described in terms of the used orbital and configuration excitation manifold.

We employed the 4s3p2d1f ANO basis set of Widmark, Malmqvist and Roos [16] for our calculations. This basis set was designed to describe ground as well as valence excited states. In order to avoid instabilities in the response calculations it is important to select a proper active space for the ground state. the active space was selected from an analysis of the occupation numbers of the second-order Møller–Plesset density matrix at the equilibrium geometry of the excited triplet state. The $1\sigma_g$ and the $1\sigma_u$ orbitals are inactive. An active space consisting of three MOs of σ_g type, two of σ_u type and one of π_g and π_u type gave a consistent cutoff between the occupation numbers of occupied and unoccupied orbitals. The ten active electrons were thus distributed in nine orbitals. Additional tests were made in order to assure the soundness of the choices of basis set and active space. In order to test the basis set convergence for the phosphorescence transition, diffuse s, p, and d functions were added, but in the relevant internuclear interval no significant changes were observed. The use of an active space consisting of nine orbitals was tested against an active set with an additional σ_g

orbital and for the interesting internuclear distances no significant changes were observed.

4. Results and discussion

A number of experimental studies of the Vegard–Kaplan band exists. Shemansky [13] measured the absorption spectrum of the transition and identified the seven vibrational bands (6, 0)–(12, 0), and extracted from these data an absolute transition moment curve in the interval 1.08–1.14 Å. The transition moment curve was found to be linear in this interval. Chandraiah and Shepherd [11] as well as Broadfoot and Maran [14] performed emission measurements of the vibrational transitions. This allowed the identification of a relative transition moment curve in the interval 1.23–1.43 Å. Shemansky [13] showed that a simple linear extrapolation of the absorption curve was consistent with the emission measurements and obtained thereby a nearly linear transition moment curve in the interval 1.08–1.43 Å. The obtained transition moment curve changes sign at 1.173 Å. The resulting transition moment curve was then used to calculate the lifetimes of the triplet state in its lowest vibrational state. For the $\Sigma = \pm 1$ components of the triplet state a lifetime of 2.5 s was deduced and for the $\Sigma = 0$ component a lifetime of 1.27 s was obtained. Similar lifetimes were concluded from Shemansky's and Carleton's reexamination [15] of an experiment by Carleton and Oldenberg [10] giving the lifetime of the $A\,^3\Sigma_u^+$ state relative to the lifetime of the $B\,^3\Pi_g$ state.

In the electric dipole approximation adopted in our work for radiative probabilities the decay from the $\Sigma = 0$ spin sublevel is forbidden. The components of the spin–orbit operator transform according to the irreducible representations Σ_g^- and Π_g of the point group $D_{\infty h}$ for the longitudinal and the perpendicular components, respectively. Interaction with a Σ_u^+ state gives total symmetries Σ_u^- and Π_u and only the latter dipole interacts with the $^1\Sigma_g^+$ ground state. So, in the electric dipole approximation only the $\Sigma = \pm 1$ components of the $A\,^3\Sigma_u^+$ state can radiate in the Vegard–Kaplan system. The Σ_u^- intermediate states ($\Sigma = 0$ spin sublevel), on the other hand, can radiate through the large SOC mixing with the $a'\,\Sigma_u^-$ state [17] and through intensity borrowing from the $a'\,^1\Sigma_u^- - X\,^1\Sigma_g^+$ transition. The latter channel is also rigorously forbidden by pure electronic selection rules, but it borrows electric dipole intensity from the $^1\Pi_u - X\,^1\Sigma_g^+$ transition through electronic–rotational perturbation, which is the cause of Λ-type doubling in $^1\Pi$ states, and of slight changes in the rotational constants [18,19]. The $\Sigma = 0$ component of the $A\,^3\Sigma_u^+$ state cannot radiate in the quadrupole approximation, but this radiation is not forbidden as a magnetic dipole transition with account for SOC or with the direct interaction between the spin and the magnetic field of the light. Anyway the $\Sigma = 0$ component of the Vegard–Kaplan system must be weaker than the $\Sigma = \pm 1$ components. Shemansky's assignment [13,15] of two different lifetimes for $\Sigma = 0$ and $\Sigma = \pm 1$ substate levels refers to the Hund's case (b) rotational line strength. Our calculations refer to pure electronic–vibrational transitions in a non-rotating molecule and predict, of course, two equal lifetimes for the $\Sigma = \pm 1$ spin substates and infinity lifetime for the $\Sigma = 0$ substate. The long lifetime of the $A\,^3\Sigma_u^+$ state (2s) guarantees that the rotational and spin structure would be in thermal equilibrium under laboratory conditions, used for the Vegard–Kaplan bands studies [9–15] and only a single thermally averaged lifetime could be measured by the observations of laboratory afterglows.

The phosphorescence transition moment curve obtained is shown in Fig. 1. While the curve obtained from experimental data is close to linear and changing sign at 1.173 Å, our curve is non-linear with the sign shift occurring at 1.175 Å. However, in the region 1.1–1.4 Å, where emission and absorption data provide information about the curve, we do observe a curve which is nearly linear. Since the vanishing of the transition moment is caused by the cancellation of a sum of terms, the exact point where this cancellation occurs is very sensitive to the accuracy of the wavefunctions. The good representation of this point seems to support the used approximations and the response theory approach. The interpolated transition moment curve obtained by Shemansky [13] is quadratic but, in the appropriate r interval, quite close to being linear. The slope of the curve is opposite to the one of Broadfoot and Maran [14] and to our curve, but the choice is arbitrary. A reexamination of both curves from Refs. [13,14] shows that at large internuclear distances ($r > 1.4$ Å) there is a change of

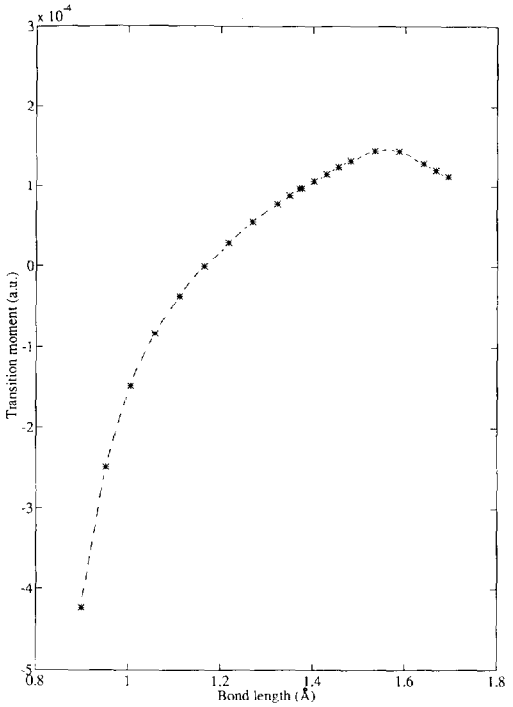

Fig. 1. The computed transition moment of the Vegard–Kaplan system.

the slope very similar to the dependence presented in Fig. 1. Comparison of the 0–11 and 0–12 transitions definitely shows the features [13,14] to be very similar to the curve given in that figure.

Because of large differences in equilibrium geometries of the singlet and triplet states, the triplet state has an equilibrium distance, which is 0.19 Å larger than the equilibrium geometry of the ground state [18], the phosphorescent transition has a rather complex vibrational structure. The lowest vibrational state of the excited triplet decays mainly to excited vibrational states of the ground state. Vibrational averages were obtained from the first vibrational state of the triplet state to the 15 lowest vibrational states of the ground state. The vibrational wavefunctions were obtained from a Morse potential curve that reproduces the spectroscopic constants. The transition rate (in s^{-1}) from vibration v' of the triplet to vibration v of the singlet is obtained as

$$A(v, v') = \tfrac{4}{3}\alpha^3 \sqrt{\frac{eh}{ma_0^2}}\, \omega_{vv'}^3\, T(v, {}^1\Sigma_g^+ \,|\, v', {}^3\Sigma_u^+)^2, \quad (9)$$

where α is the fine structure constant, e is the charge of the electron, h is Planck's constant, m is the mass of the electron and a_0 is the atomic unit of length. The transition energy in atomic units is given by $\omega_{v,v'}$ and $T(v, {}^1\Sigma_g^+ \,|\, v', {}^3\Sigma_u^+)$ is the vibrationally averaged transition moment in atomic units. Since higher vibrational states are important it was necessary to include both electronic and vibrational energies in the energy term in the above equation. In Table 1 we report the Einstein coefficients for emission from the lowest vibrational state of the triplet as well as the values reported by Shemansky [13] scaled so that the spin-sublevel averaged emission is obtained. The experimental and theoretical relative intensities are in qualitative agreement, but the absolute theoretical intensity is systematically underestimated. Relative vibronic probabilities agree much better with experiment. Both the theoretical and experimental data show the largest intensity for the bands with $v = 6, 7$. Since the relative intensities of the higher vibrations are very sensitive to the transition moment curve, the small deviations in relative vibronic transition probabilities are not surprising.

The total transition rate of a given vibrational state v' of the triplet is obtained as $A(v') = \sum_v A(v, v')$ and the lifetime is equal to $1/A(v')$. From the data of Ta-

Table 1
Theoretical and experimental Einstein coefficients (s^{-1}) for the spin-sublevel averaged emission from the lowest vibration state of $^3\Sigma_u^+$ state to the vibrational states v of the ground $X\ ^1\Sigma_g^+$ state

v	Theoret. rate	Exp. rate [a]
0	0.000007	0.000003
1	0.0005	0.0004
2	0.0037	0.0043
3	0.0134	0.0195
4	0.0304	0.0505
5	0.0472	0.0872
6	0.0534	0.1089
7	0.0474	0.1025
8	0.0331	0.0750
9	0.0177	0.0435
10	0.0075	0.0203
11	0.0027	0.0077
12	0.0008	0.0024
13	0.0002	0.0006

[a] From Table 6 of Ref. [13]. The numbers are multiplied by $\frac{2}{3}$ for spin-sublevel averaging.

ble 1, a total rate of 0.387 s^{-1} and a lifetime of 2.58 s are predicted for one of the $\Sigma=1$ spin sublevels. In the rotationless molecule the $\Sigma=0$ sublevel does not radiate, so the averaged radiative lifetime,

$$\frac{3}{\tau_{av}} = \sum_{\Sigma} \frac{1}{\tau_{\Sigma}}, \tag{10}$$

is equal to $\frac{3}{2}\tau_{\Sigma=1}=3.87$ s. Considering that the values of Shemansky [9] should be averaged, the lifetime is 1.9 s. The calculated value is thus approximately twice as large as the experimental lifetime. We should also mention that the nature of averaging is rather different because Shemansky has calculated lifetimes for the rotational sublevels and we have considered a nonrotating molecule. Shemansky's conclusion about the most intensive transition for the $\Sigma=0$ component came from an analysis of rotational lines strengths in the absorption spectrum [13]. The analysis was based on several assumptions in assessing the contributions of the four rotational branches (P_2, Q_1, Q_3 and R_2) to the band transition probability, including the simplifying approximation of the pure Hund's case (b) coupling. Shemansky argued that little difference in the eigenfunctions of the three spin substates can be expected since the $A\,^3\Sigma_u^+$ state very nearly follows Hund's coupling case (b), and the substates are therefore almost degenerate [13]. However, one must remark here that the small splitting of the spin substates does not mean a small difference in their electronic eigenfunctions and in their intrinsic ability for spontaneous radiation; the splitting of $^3\Sigma$ state is determined by the weak spin–spin coupling to first order and by SOC to second order in perturbation theory [20]. The SOC contribution to the spin splitting of the $A\,^3\Sigma_u^+$ state is mainly determined by small singlet–triplet splitting of the $a'\,^1\Sigma_u^-$ and the $B'\,^3\Sigma_u^-$ states [20]. The singlet–triplet transition intensity on the other hand is determined by the first-order SOC and has a completely different origin. The eigenfunctions of the $\Sigma=\pm1$ sublevels of the $A\,^3\Sigma_u^+$ state have quite large singlet state $^1\Pi_u$ contaminations, while the $\Sigma=0$ sublevel has only the $^1\Sigma_u^-$ admixtures, which do not provide any electric dipole activity. Near degeneracy of spin sublevels of the $A\,^3\Sigma_u^+$ state does not mean that their radiative transition probabilities to the ground state would be similar. Even if Shemansky's analysis of rotational line intensities in the Vegard–Kaplan system is correct we should like to mention the following. The fundamental properties of a molecule are determined by its electronic shell peculiarities, not by rotation. We obtained the two radiative lifetimes for the $A\,^3\Sigma_u^+$ state in a non-rotating N_2 molecule as: $\tau(\Sigma=0)=\infty$, $\tau(\Sigma=\pm1)=2.58$ s. The averaged lifetime for the fast spin–lattice relaxation limit (sublevel population equalized by collision), which only could be measured in gas-phase discharge ($1.5\tau(\Sigma=\pm1)=3.87$ s), differs significantly from Shemansky's spin-averaged estimation (1.9 s) [13], though the value $\tau(\Sigma=\pm1)$ coincides occasionally with Shemansky's result (2.5 s). This occasional coincidence was somewhat misleading for the authors. It is quite natural to estimate the rotational lines intensities in N_2 absorption, but it is somewhat artificial to analyze the spin-rotational level lifetimes, because they decay with the averaged rate in gas phase discharge. It is possible to resolve the decay from a different spin sublevel in low-temperature crystals, but in this case the rotation is suppressed.

Because the radiative lifetimes of the rotated spin sublevels inferred by Shemansky [13] could not be verified by direct real afterglow measurement (it needs unattainable low pressure) we also tried to compare our results with other experimental works. Most of the earlier measurements of the lifetime appear to be rather uncertain, see for example discussions in Refs. [9,15]. Because of the small radiative probability, direct measurements in the gas-phase discharge are very difficult. Noxon [9] has presented convincing arguments for the averaged lifetime of roughly 1 s, based on his afterglow measurements at 1 atm pressure. This was a direct estimation, which was not connected with any fine spectroscopic features and speculations. Carleton and Oldenberg [10] carried out direct measurements of the $A\,^3\Sigma_u^+$ state population (by the triplet–triplet absorption calibration in the first negative system) and the volume absolute emission rate. They widened the slit of the spectrograph until the rotational structure of the Vegard–Kaplan band was unresolved and obtained the averaged radiative lifetime in the level $v=0$ of the $A\,^3\Sigma_u^+$ state to be 2 ± 0.9 s. Another important result has been obtained by Tinti and Robinson [12]. They measured the lifetime of the $A\,^3\Sigma_u^+$ state in different solid rare gases at 1.7–4.2 K and obtained 0.4 s in Ar and 3.3 s in Ne matrices. The latter value was claimed

to be close to the gas-phase value. Since $v' > 0$ are not seen at this temperature for Ne host, the decay is not affected by slow vibrational cascading, as it is in the gas phase [12]. We suppose that spin–lattice relaxation is very slow and rotation is suppressed at these conditions. The important result of Ref. [12] is that the initial decay is exponential, which would be improbable if the two spin sublevels should have two different finite values of the same order in a nonrotating molecule. Moreover, a very long-lived nonexponential tail is presented on the decay curve (Fig. 6 of Ref. [12]). It should correspond to the $\Sigma=0$ spin sublevel with $\tau > 100$ s. This tail does not contribute appreciably to the initial decay, which was taken to be the 'lifetime' of the $A\,^3\Sigma_u^+$ state in the Ne host [12]. Tinti and Robinson proposed that the tail most likely arises from $N(^4S)$ atom recombination in the solid, which repopulates the $A\,^3\Sigma_u^+$ state after the excitation is switched off. The host environment definitely should enhance the forbidden emission from the $\Sigma=0$ sublevel, so the lifetime of the order of few hundred seconds is easily accessible [18]. In order to check this proposal it would be desirable to carry out an ODMR experiment for N_2 in rare gas matrices.

Finally, we have estimated the radiative lifetime of the $\Sigma=0$ spin sublevel beyond the electric dipole approximation in a semi-empirical way [17]. Because of the large SOC matrix element $\langle A\,^3\Sigma_{u,0}^+ | H_{so} | a'\,^1\Sigma_u^- \rangle = 0.5\zeta_N = 36\ cm^{-1}$, where ζ_N is the SOC constant of the nitrogen atom, the $\Sigma=0$ spin sublevel in the Vegard–Kaplan transition can borrow intensity from the Ogawa–Tanaka–Wilkinson–Mulliken band $a'\,^1\Sigma_u^- \rightarrow X\,^1\Sigma_g^+$. Taking into account the oscillator strength of this band from experiment ($f = 6.54 \times 10^{-10}$, which corresponds to the lifetime 0.5 s [18]), we can estimate the lifetime of the $\Sigma=0$ sublevel of the $A\,^3\Sigma_u^+$ state as being equal to 584000 s. The direct interaction of the spin with the magnetic component of the light field cannot provide a large transition probability because of the small size of the N_2 molecule. We cannot see other sources for the transition probability for the $\Sigma=0$ component of the Vegard–Kaplan system.

5. Summary

The transition moment curve of the Vegard–Kaplan band has been obtained by employing quadratic response theory at the MCSCF level. Employing a complete active expansion of the ground state reference wavefunction, the obtained transition moment curve is in good agreement with the experimental curve, but our calculations give somewhat less intensive transitions at large distances. At small distances ($r < 1.2$ Å) the two curves are quite close, with the transition moment vanishing at an internuclear distance of 1.17 Å. A qualitative agreement is obtained for the transition rates from the lowest triplet vibrational state to the vibrational states of the ground state. both theory and experiment show that the transitions to the ground state vibrations with $v = 6, 7$ are the most intensive ones.

We calculate a spin averaged lifetime of 3.87 s for the first vibrational level of the triplet state, which is fairly close to the range of experimental estimations (1–3.3 s) and two times as large as the most reliable value of 1.9 s [13]. We stress that the calculated electric dipole transition moment for the $\Sigma = \pm 1$ sublevels and relative intensities of different vibronic transitions coincides quite well with the experimentally derived quantities. We finally note that the collision-induced enhancement of the Vegard–Kaplan transition probability has not yet been studied.

Acknowledgement

This work was supported by grants from the Swedish and Danish natural science research councils (NFR and SNFR), from the Swedish Royal Academy of Sciences, from the Nordic council of ministers through the NORFA network, and from CRAY Research Inc. Patrick Norman and Dan Jonsson are acknowledged for performing additional calculations.

References

[1] S. Wilson, ed., Methods in computational chemistry, Vol. 2. Relativistic effects in atoms and molecules (Plenum Press, New York, 1988).
[2] M.R. Manaa and D.R. Yarkony, J. Chem. Phys. 95 (1991) 1808.
[3] S.R. Langhoff and E.R. Davidson, J. Chem. Phys. 64 (1976) 4699.
[4] M.R. Manaa and D.R. Yarkony, J. Chem. Phys. 95 (1991) 6562.

[5] O. Vahtras, H. Ågren, P. Jørgensen, H.J.Aa. Jensen and J. Olsen, J. Chem. Phys. 97 (1992) 9178.
[6] J. Olsen and P. Jørgensen, J. Chem. Phys. 82 (1985) 3235.
[7] H.J.Aa. Jensen, P. Jørgensen, H. Hettema and J. Olsen, Chem. Phys. Letters 187 (1991) 387.
[8] H. Hettema, H.J.Aa. Jensen, P. Jørgensen and J. Olsen, J. Chem. Phys. 97 (1992) 1174.
[9] J.F. Noxon, J. Chem. Phys. 36 (1962) 926.
[10] N.P. Carleton and O. Oldenberg, J. Chem. Phys. 36 (1962) 3460.
[11] G. Chandraiah and G.G. Shepherd, Can. J. Phys. 46 (1968) 221.
[12] D.S. Tinti and G.W. Robinson, J. Chem. Phys. 49 (1968) 3229.
[13] D.E. Shemansky, J. Chem. Phys. 51 (1969) 689.
[14] A.L. Broadfoot and S.P. Maran, J. Chem. Phys. 51 (1969) 678.
[15] D.E. Shemansky and N.P. Carleton, J. Chem. Phys. 51 (1969) 682.
[16] P.O. Widmark, P.-Å. Malmqvist and B.O. Roos, Theoret. Chim. Acta 77 (1990) 291.
[17] B.F. Minaev, J. Mol. Struct. THEOCHEM 183 (1989) 207.
[18] A. Lofthus and P.H. Krupenie, J. Phys. Chem. Ref. Data 6 (1977) 113.
[19] P.G. Wilkinson and R.S. Mulliken, J. Chem. Phys. 31 (1959) 674.
[20] B.F. Minaev, Ph.D. Thesis, Tomsk University, Tomsk (1973).